International Journal of Electrical and Computer Engineering (IJECE)
Vol. 15, No. 3, June 2025, pp. 2769~2785
ISSN: 2088-8708, DOI: 10.11591/ijece.v15i3.pp2769-2785

The implementation of Archimedes optimization algorithm for solar charge controller-maximum power point tracking in partial shading condition

Sigit Dani Perkasa[1], Prisma Megantoro[1], Nayu Nurrohma Hidayah[1], Pandi Vigneshwaran[2]
[1]Faculty of Advanced Technology and Multidiscipline, Universitas Airlangga, Surabaya, Indonesia
[2]Department of Computer Science and Engineering, Acharya University, Karakul, Uzbekistan

Article Info

Article history:

Received Aug 19, 2024
Revised Jan 17, 2025
Accepted Mar 3, 2025

Keywords:

Archimedes optimization algorithm
Embedded system
Maximum power point tracking
Photovoltaic
Renewable energy
Solar energy

ABSTRACT

Maximum power point tracking (MPPT) enhances the efficiency of solar photovoltaic (PV) systems by ensuring optimal power extraction under varying conditions. MPPT is implemented in solar charge controllers or hybrid inverters connected to PV arrays. The current-voltage (IV) curve, influenced by temperature and irradiance fluctuations, becomes more complex under partial shading, causing multiple local maxima and reducing efficiency. This study proposes an MPPT technique using the Archimedes optimization algorithm (AOA), a novel metaheuristic inspired by Archimedes' principle. The AOA-based MPPT integrates a DC/DC buck converter controlled by an STM32 microcontroller to address challenges in complex shading conditions. Comparative analysis demonstrates the AOA's superiority in achieving high efficiency and fast convergence. The AOA-based MPPT achieved an average efficiency of 93.17% across shading scenarios, outperforming PSO (87.04%) and non-MPPT systems (84.56%). It also exhibited faster average tracking times of 90.5 ms compared to PSO's 100.5 ms, ensuring robust and reliable performance. These results confirm the effectiveness of the AOA-based method in maximizing energy harvesting in real-world PV applications.

Corresponding Author:

Prisma Megantoro
Faculty of Advanced Technology and Multidiscipline, Universitas Airlangga
60115 Surabaya, Indonesia
Email: prisma.megantoro@ftmm.unair.ac.id

1. INTRODUCTION

The global energy landscape is rapidly shifting towards renewable energy sources, with solar photovoltaic (PV) systems playing a crucial role in this transition due to their potential for large-scale deployment and sustainability [1]. However, the efficiency of PV systems is significantly hampered by partial shading conditions, which cause multiple local maxima on the power-voltage (P-V) curve, complicating the process of maximum power point tracking (MPPT) and leading to suboptimal energy extraction [2], [3]. The development and implementation of advanced MPPT algorithms are therefore essential to ensure that PV systems operate at their maximum potential under varying environmental conditions [4]–[6].

Traditional MPPT algorithms, such as perturb and observe (P&O) and incremental conductance (INC), have been widely adopted due to their simplicity and ease of implementation [7], [8]. Some researchers used fuzzy-based optimization for the MPPT implementation [9]–[13]. However, these methods often suffer from drawbacks such as oscillations around the maximum power point (MPP) and reduced accuracy under rapidly changing environmental conditions, particularly in partial shading conditions [14]–[16]. Moreover, while these techniques perform adequately under uniform irradiation, their effectiveness significantly diminishes in non-uniform conditions, leading to increased power losses and inefficiencies in energy harvesting [17]–[20].

To overcome these challenges, recent advancements have seen the introduction of bio-inspired and metaheuristic algorithms, such as the cuckoo search (CS) [21], seagull optimizer (SO) [22], and spotted hyena optimizer (SHO) [23], squirrel search algorithm (SSA) [24], mutant particle swarm optimization (MPSO) [25], modified particle swarm optimization (PSO) [26], fusion firefly algorithm (FFA) [27], an immune firefly algorithm (IFA) [28], grey wolf optimization (GWO) [29], Harris hawk optimization (HHO) [30], moth flame optimization (MFO) [31], grasshopper optimization (GHO) [32], and ant colony optimization (ACO) [33]. These algorithms offer improved tracking performance by more effectively navigating the complex P-V landscapes caused by partial shading conditions (PSCs) also Zafar *et al.* [34] wrote a novel about MPPT control techniques for PV systems under partial shading conditions using the metaheuristic algorithm.

Megantoro *et al.* [35] conducted research to compare some evolutionary algorithms (EA), such as the genetic algorithm (GA), firefly algorithm (FA), fruitfly algorithm (FOA), and PSO, which are also used for solving the MPPT problem in partial shading conditions. These algorithms have demonstrated superior convergence speed, accuracy, and robustness compared to conventional methods, making them highly promising for real-world applications [36].

Recent advancements in optimization algorithms have opened new avenues for tackling the challenges of partial shading in photovoltaic (PV) systems. The archimedes optimization algorithm (AOA) has emerged as a promising metaheuristic method due to its dynamic balance between exploration and exploitation, efficient convergence capabilities, and adaptability to complex optimization problems. AOA's versatility has been demonstrated in various domains, including optical system design, where it achieved superior optimization outcomes in intricate tasks [37]. It has also been successfully applied to optimize variable pitch wind turbine control, handling multifaceted engineering challenges [38]. In the renewable energy sector, AOA has shown excellent performance in MPPT under partial shading conditions, delivering higher efficiency and faster convergence than traditional methods [39]. Additionally, AOA has been utilized in power systems optimization, such as PID tuning of a DC-DC buck converter [40] and optimizing power flow in electrical systems from optimal electric vehicle charging station placement [41]. These applications underscore AOA's robustness and efficiency, justifying its use in this study to address the complex, nonlinear power-voltage landscapes of PV systems affected by partial shading. This research aims to build upon these proven strengths of AOA to enhance MPPT performance and ensure optimal energy harvesting under challenging environmental conditions.

This study introduces the AOA as an approach to MPPT in PV systems under partial shading conditions, addressing the challenges of complex power-voltage landscapes. Integrating AOA into a real-time embedded system with a DC/DC buck converter highlights its practical applicability and scalability for low-cost PV solutions. The study combines rigorous simulation and real-world validations to establish the algorithm's reliability and adaptability. Furthermore, this research lays the foundation for extending AOA to broader renewable energy applications, offering a cutting-edge solution for dynamic and nonlinear optimization problems.

2. METHOD

This section explains the methods used in the research. The designed MPPT device used a simulated model of a PV module in different partial shading conditions that act as the power supply for the whole system. At the same time, the MPPT itself is a combination of an SCC DC/DC buck converter controlled with a microcontroller injected with the AOA.

2.1. Partial shading PV simulation model

Partial shading in PV modules significantly affects the performance and efficiency of solar energy systems. When a PV module is partially shaded, the output power of the entire string of PV modules can be significantly reduced. Partial shading also creates multiple peaks in the power-voltage (P-V) characteristic curve of the PV system, complicating the task of MPPT [42]. Simulation tools like MATLAB and PSIM have been used to model and analyze the effects of partial shading to help understand the I-V (current-voltage) and P-V characteristics of solar modules under non-uniform irradiation [43], [44].

The photovoltaics module in this research simulated four variations of partial shading conditions: full irradiance, quarter-shaded, half-shaded, and quarter-irradiance. The simulation was conducted with the help of IT-M3622 Bi-Directional Power Supply and SAS1000 Software, both of which are manufactured by ITECH. The IT-M3622 supplies physical voltages and current as an actual PV module, paired with SAS1000 that runs the PV module specifications, shadow quantities and movement variations, and data acquisition. The ITECH

IT-M3622 power supply simulates an 80 Wp PV module in different scenarios of partial shading conditions from the shadow mode of SAS1000 software with the shading configuration illustrated in Figure 1.

2.2. MPPT technique

MPPT is a crucial technique used in photovoltaic (PV) systems to optimize power extraction from solar panels by ensuring they operate at their MPP. Since environmental factors such as solar irradiation and temperature continuously fluctuate, the MPP varies. It is requiring dynamic adjustments to maintain maximum efficiency. MPPT algorithms continuously track these changes and adjust the operating voltage or current to ensure optimal power output.

The simulated partial shading configuration in Figure 1 consisted of 4 shadow conditions covering different areas of the simulated 36 cells' PV module, representing eight small rectangles of 4.5 cells each. In Figure 1(a), the PV cells are completely irradiated, while in Figure 1(b), 25% of the upper-left PV cells are shaded, and only 27 cells are irradiated. In Figure 1(c), the half-left of the PV cells ware covered, and only 18 cells were irradiated, and in Figure 1(d), only nine cells in the lower-right are irradiated or 75% shaded.

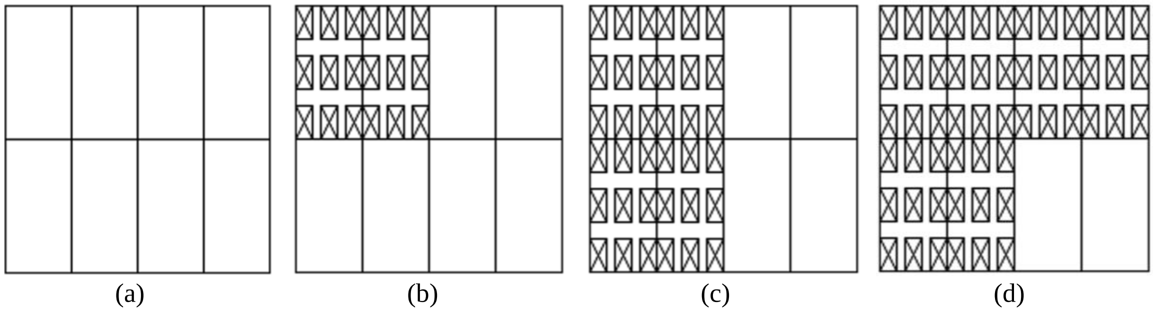

Figure 1. PV module shading configuration; (a) 100% irradiance, (b) 75% irradiance, (c) 50% irradiance, and (d) 25% irradiance

2.3. Archimedes optimization algorithm

The AOA is a novel metaheuristic algorithm inspired by Archimedes' principle [42], [43]. The AOA's agents significantly advance optimization, leveraging physical principles to enhance computational efficiency and solution quality [44], [45]. The AOA is classified into six mathematical steps in this research, which are explained in the following section.

The AOA was chosen for this study due to its ability to optimize complex, nonlinear systems effectively. Unlike traditional algorithms such as PSO or GA, AOA's dynamic balance between exploration and exploitation enables it to converge faster while avoiding local optima. Recent applications of AOA further underscore its versatility and efficiency. For instance, AOA has been employed in renewable energy optimization and power systems engineering, achieving superior performance metrics [37], [39]–[41], [45]–[49]. These merits make AOA a compelling choice for addressing the challenges of MPPT under partial shading conditions.

2.3.1. Initialization

In this step, object positions are initialized using (1). Where O_i represents the *i*-th object in a population of *N*. lb_i and ub_i denote the lower and upper bounds of the search range, respectively. The initialization of volume (*vol)* and density (*den*) for each object *i* follows (2).

$$O_i = lb_i + rand \times (ub_i - lb_i); i = 1, 2, ..., \tag{1}$$

with *rand* is a dimensional vector *D* randomly generating numbers between 0 and 1. The velocity (*acc)* is initialized using (3). In this step, the initial population is evaluated, and the object with the best fitness value is chosen and added to x_{best} , $den_{best}, vol_{best}, acc_{best}$ variables.

$$den_i = rand;\ vol_i = rand \tag{2}$$

$$acc_i = lb_i + rand \times (ub_i - lb_i) \tag{3}$$

2.3.2. Updating density and volume

The density and volume of the *i*-th object for iteration number t + 1 were updated using (4) and (5). Where den_{best} and vol_{best} is the density and volume of the best object found with uniform *rand.*

$$den_i^{t+1} = den_i^{t+1} + rand \times (den_{best} - den_i^1) \tag{4}$$

$$vol_i^{t+1} = vol_i^{t+1} + rand \times (vol_{best} - vol_i^1) \tag{5}$$

2.3.3. Transfer operator and density factor

Collisions among objects occur, and over time, these objects attempt to reach an equilibrium point. The transfer function (TF) required for transforming the search from exploration to exploitation is defined in (6). *TF* increases with time until reaches 1, while *t* and t_{max} is iteration number and maximum iteration. Density decreasing factor (*d)* helps AOA move from global search to local search, which decreases with time according to (7).

$$TF = \exp\left(\frac{t-t_{max}}{t_{max}}\right) \tag{6}$$

$$d^{t+1} = \exp\left(\frac{t_{max}-t}{t_{max}}\right) - \left(\frac{t}{t_{max}}\right) \tag{7}$$

2.3.4. Exploration and exploitation

a. Exploration phase (object collisions)

If *TF* ≤ 0.5, collisions between objects happen, and random material (*mr)* is selected, and object acceleration is updated using (8). Where den_i, vol_i, and acc_i is the density, volume, and velocity of the *i*-th object. While den_{mr}, vol_{mr} and acc_{mr} is the density, volume, and velocity of the randomly selected object.

$$acc_i^{t+1} = \frac{den_{mr}+vol_{mr}\times acc_{mr}}{den_i^{t+1}\times vol_i^{t+1}} \tag{8}$$

b. Exploitation phase (no object collisions)

Suppose *TF* > 0.5; collisions between objects do not happen. Object velocity at *t* + 1 is updated using (9). Where acc_{best} is the velocity of the best object.

$$acc_i^{t+1} = \frac{den_{best}+vol_{best}\times acc_{best}}{den_i^{t+1}\times vol_i^{t+1}} \tag{9}$$

2.3.5. Normalizing acceleration

Velocity is normalized to compute percentage change using (10). Where *u* and *l* are the normalization range set to 0.9 and 0.1, respectively. acc_{i-norm}^{t+1} determines the step percentage change for each agent. Objects far from the global optimal value will have higher velocity values, indicating the transition from the exploration phase to the exploitation phase.

$$acc_{i-norm}^{t+1} = u \times \frac{acc_i^{t+1}-\min(acc)}{\max(acc)-\min(acc)} + l \tag{10}$$

2.3.6. Position update

In the exploration phase, the position of the *i*-th object in iteration number *t* + 1 is updated using (11). Where C_1 is a constant equal to 2, in the exploitation phase (*TF* > 0.5), the object position is updated using (12).

$$x_i^{t+1} = x_i^t + C_1 \times rand \times acc_{i-norm}^{t+1} \times d \times (x_{rand} - x_i^t) \tag{11}$$

$$x_i^{t+1} = x_{best}^t + F \times C_2 \times rand \times acc_{i-norm}^{t+1} \times d \times (T \times x_{best} - x_i^t) \tag{12}$$

where C_2 is equal to 6, T increases linearly with time and is proportional with TF and defined with $T = C_1 \times TF$ with a range of $C_3 \times 0.3$ to 1. Object movement direction changes are represented as F in (13). Where $P = 2 \times rand - C_4$

$$F = \begin{cases} +1 \ if \ P \leq 0.5 \\ -1 \ if \ P > 0.5 \end{cases} \tag{13}$$

2.3.7. Objective function

The objective function of the proposed system aims to optimize the duty cycle (D), representing the population (X) in AOA, to maximize the power output (P_{out}). Each candidate duty cycle corresponds to a PWM value controlling the DC/DC buck converter, and the AOA iteratively adjusts these values to find the global MPP under partial shading. The objective function is represented by (14).

$$F(X) = V_{out} \cdot I_{out} \tag{14}$$

where X=D (duty cycle), V_{out} is the MPPT output voltage, and I is the MPPT output current. By dynamically evaluating and refining the duty cycle, the AOA ensures the PV system operates efficiently, adapting to complex and changing environmental conditions.

2.3.8. AOA parameters

The performance of the AOA in MPPT applications depends heavily on adequately tuning its parameters. These parameters govern the algorithm's ability to balance exploration and exploitation, ensuring efficient and accurate convergence to the global MPP for MPPT in photovoltaic PV systems, the parameters have been tuned to suit dynamic and partial shading conditions, as detailed in Table 1. By setting these parameters appropriately, the AOA can dynamically adapt to changes in irradiance and shading conditions, ensuring robust MPPT performance. The chosen values balance computational efficiency and optimization precision, making the AOA suitable for real-time embedded applications in PV systems.

Table 1. AOA tuning parameters

Parameter	Value
Population Size (N)	20
Maximum Iterations (T_{max})	50–100
Initial Density (den_{init})	0.1–0.9
Initial Volume (Vol_{init})	0.1–0.9
Transfer Function (*TF*)	0 to 1
Acceleration Coefficients (*C1, C2*)	C1=2.0, C2=1.0
Normalization Range (*u, l*)	*u*=0.9, *l*=0.1

2.4. SCC DC/DC buck converter

The design and implementation of solar charge controller (SCC) utilizing DC/DC buck converters play a crucial role in efficient management and storage of solar energy. The configuration of the DC/DC buck converter includes; MOSFETs, diodes, inductors, and capacitors. The configuration of the components allow efficient energy conversion by reducing the higher and fluctuating input voltages to lower and stable output voltage suited for charging batteries or powering loads [50].

3. IMPLEMENTATION

The methodology described in the previous subsection was implemented on a hardware platform to validate its practical feasibility. This implementation includes the design of a SCC to enhance power conversion efficiency. The implementation conducted along with the integration of a MPPT algorithm capable of handling partial shading conditions. Additionally, the approach for embedding the AOA into the MPPT hardware is discussed in the following subsection. It is ensuring real-time adaptability and efficient power extraction.

3.1. MPPT in partial shading

Detecting partial shading occurrences accurately is essential for initiating the appropriate MPPT response. The system integrates the selected MPPT algorithm (in this case, AOA), and their performance is tested under controlled partial shading scenarios. Data from the experiments are analyzed to verify the simulation outcomes, ensuring that the MPPT strategies are effective in real-world applications. PV output under partial shading condition simulations is represented in a set of P-V and I-V curves illustrated in Figures 2(a) to 2(d).

The I-V and P-V curves for the simulated PV module under different shading conditions in Figure 2 demonstrate the challenges and importance of MPPT in partial shading scenarios. As shading increases (from 100% to 25% irradiation) in Figure 2(a) shows the PV response in uniform insolation, Figure 2(b) shows the PV response at 75 % shading, Figure 2(c) shows the PV response at 50 % shading, and Figure 2(d) shows the PV response at 25 % shading. The curves show a reduction in both current and power output, with the introduction of multiple local maxima. This complexity requires advanced MPPT algorithms to accurately distinguish and track the true MPP among these local peaks, ensuring optimal energy harvesting.

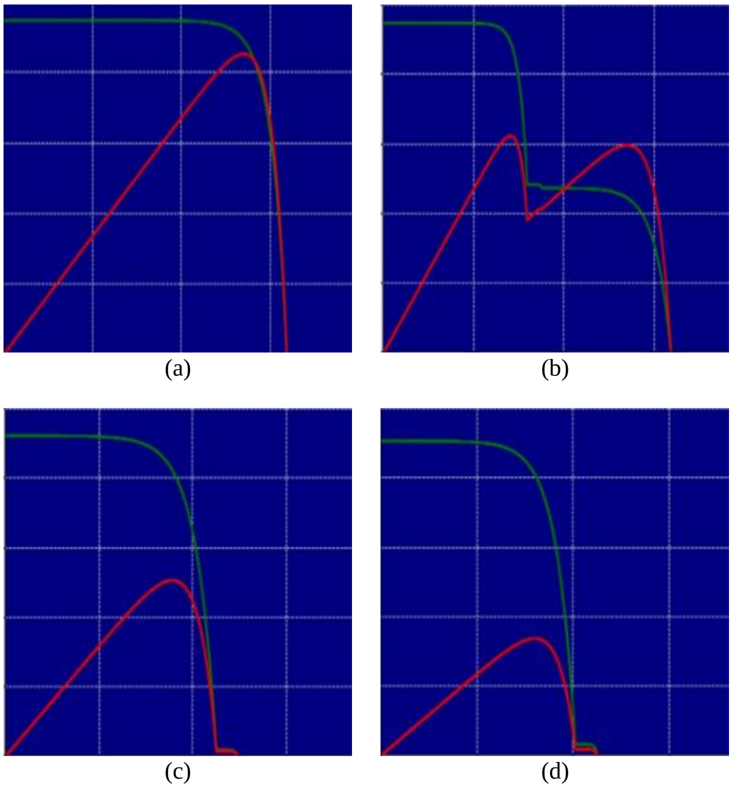

Figure 2. I-V and P-V curves of simulated PV module output under different shading conditions. (a) 100% irradiance, (b) 75% irradiance, (c) 50% irradiance, and (d) 25% irradiance

3.2. MPPT-AOA approach

In the flowchart in Figure 3, voltage and current from the PV panels are measured and fed into the MPPT algorithm. The AOA was implemented to perform a maximum of 50 iterations, generating four materials within a search range of 0 to 100, with acceleration coefficients C3=2 and C4=1, and follows the flowchart in Figure 3. The AOA optimizes the converter's duty cycle, generating a PWM signal. This PWM signal is then used to evaluate the MPP. If the optimal MPP is achieved, the process outputs it; otherwise, it loops back to optimize the tracking further.

The material generation process was evaluated, and Figure 4(a) shows significant changes in material generations from initialization to the 50th iteration, indicating AOA's dynamic and nonlinear behavior. This behavior leads to variations in material properties as AOA explores different regions of the parameter space. Following material generation, AOA updated the best material at each iteration, with the results shown in Figure 4(a) indicating convergence marked by stable PWM values. The updated material indices were input into the objective function to facilitate MPP detection, as shown in Figure 4(b). Each objective value increased until stabilizing, signifying optimal objective values achieved in the main loop. The convergence process, illustrated in Figure 4(c), shows the AOA function test results, with the algorithm achieving convergence by the 19th iteration using the specified parameters. The steps demonstrated in Figures 3 and 4 show the MPPT-AOA function's effectiveness in tracking the MPP in the solar power system, confirming AOA's capability in optimizing PV module performance under varying conditions.

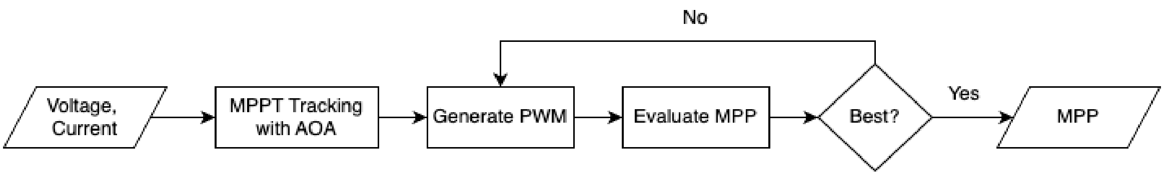

Figure 3. MPPT implementation flowchart

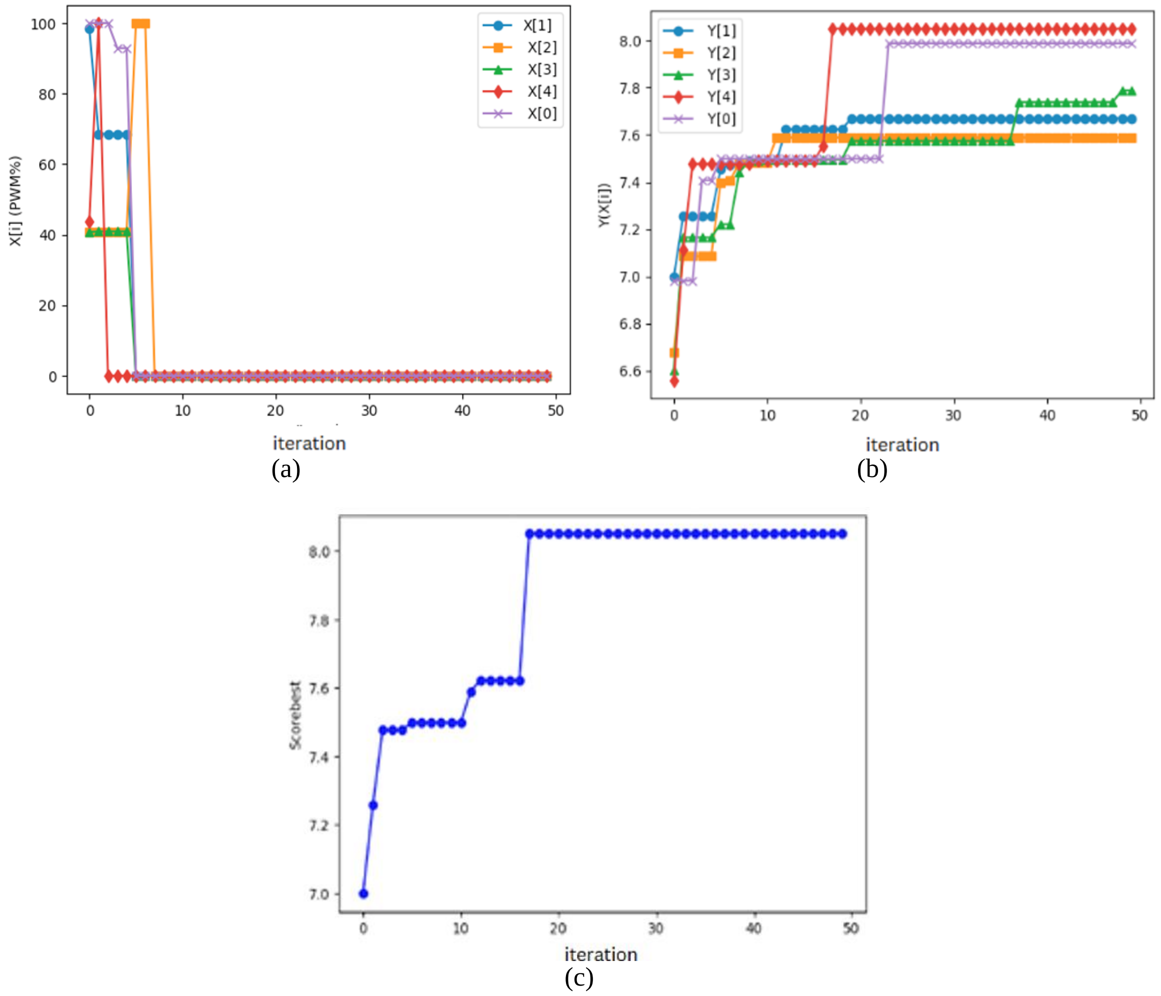

Figure 4. AOA progression of generating the best solution for each iteration. (a) material (PWM) generation, (b) objective value (MPP), and (c) AOA convergence curve

4. RESULT AND DISCUSSION

4.1. Devising the MPPT-AOA

The development of the system requires a comprehensive approach that integrates both hardware and firmware to achieve optimal performance and efficiency. The hardware design focuses on implementing key components such as power converters and control circuits. Simultaneously, the firmware design involves developing algorithms for MPPT using the AOA to enhance it with real-time adaptability and precision. The following subsections provide a detailed explanation of the methodologies used in designing both hardware and firmware.

4.1.1. Hardware design

The hardware design, as shown in Figure 5, revolves around a Nucleo-F446RE microcontroller that interfaces with essential components such as a voltage sensor (WCS1800 Module), an LCD screen (HD44780), and a power management circuit using an MP1584 buck converter. This design facilitates real-time data acquisition, allowing the microcontroller to adjust the PWM signal for optimal power output. The system also includes protection circuits to prevent overcurrent and overvoltage, ensuring reliable operation.

4.1.2. Firmware design

The firmware design of the device is illustrated in the flowchart in Figure 6. The process showed in Figure 6 starts with the configuration of peripherals, followed by obtaining the PV parameters. The system then sets the PWM based on the initial conditions and calculates AOA. If convergence to the MPP is not achieved, the object is regenerated, and the process loops until convergence is reached. Once the MPP is attained, the PWM is adjusted to maintain the system at this optimal point.

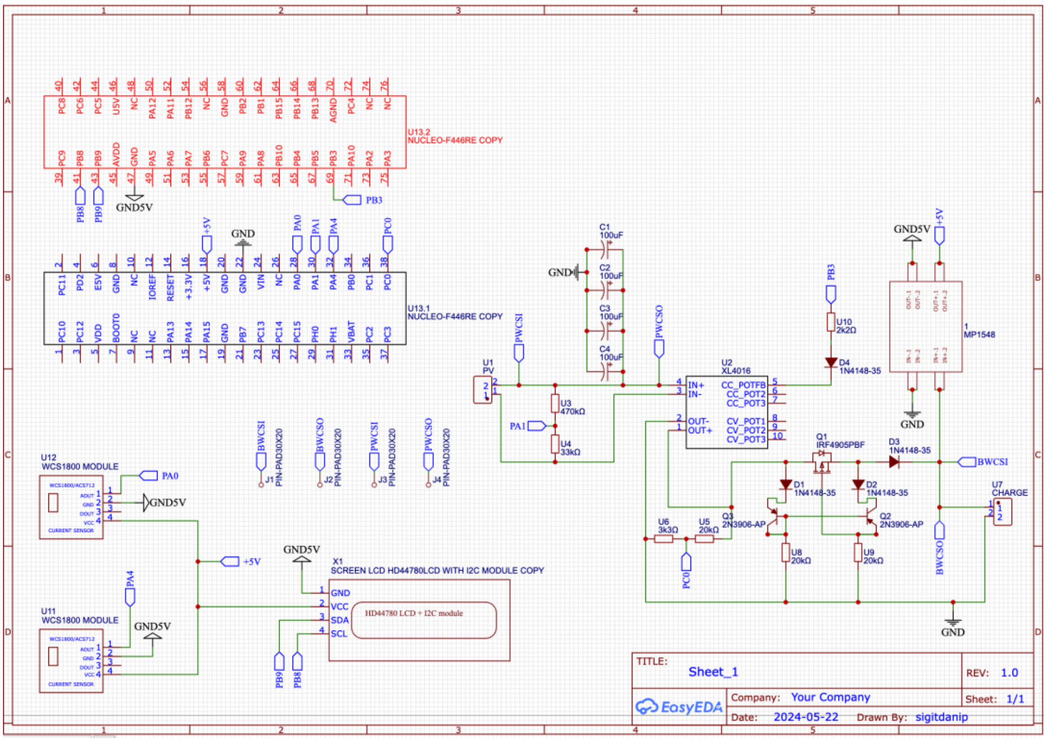

Figure 5. Hardware schematic

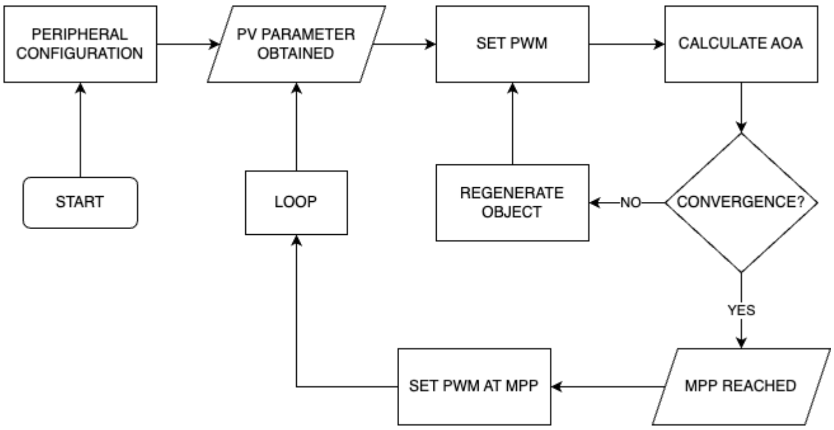

Figure 6. Flowchart of the designed firmware

4.2. MPPT-AOA performance analysis

This section presents a detailed analysis of the MPPT using the AOA under different shading conditions to assess its adaptability and efficiency. The study examines key performance aspects, including the algorithm's convergence speed, tracking accuracy, and power harvesting efficiency. The analysis aims to evaluate the robustness of MPPT-AOA in maintaining optimal PV power output despite in partial shading effects.

4.2.1. Convergence analysis

Convergence analysis is critical in determining how quickly and accurately the MPPT-AOA can reach the MPP under different shading conditions. Figure 7 illustrates the convergence behavior at different shading levels: 0%, 25%, 50%, and 75%. Under 0% shading, as shown in Figure 7(a), the algorithm exhibits a smooth and rapid convergence to the MPP, indicative of its ability to track the optimal power point in ideal conditions efficiently. When shading is introduced at 25%, as shown in Figure 7(b), the convergence process shows minor fluctuations but still manages to stabilize quickly, demonstrating the algorithm's adaptability to changes in irradiation. As shading increases to 50% in Figure 7(c), the convergence process encounters more pronounced oscillations before stabilizing, reflecting the algorithm's challenge in navigating through multiple local maxima introduced by partial shading. Under 75% shading in Figure 7(d), the convergence becomes slower and more erratic, with more significant fluctuations, yet the algorithm eventually stabilizes, albeit with reduced speed and efficiency. This analysis highlights the MPPT-AOA's capability to adapt across varying shading scenarios, though with a trade-off in convergence speed and stability as shading becomes more intense.

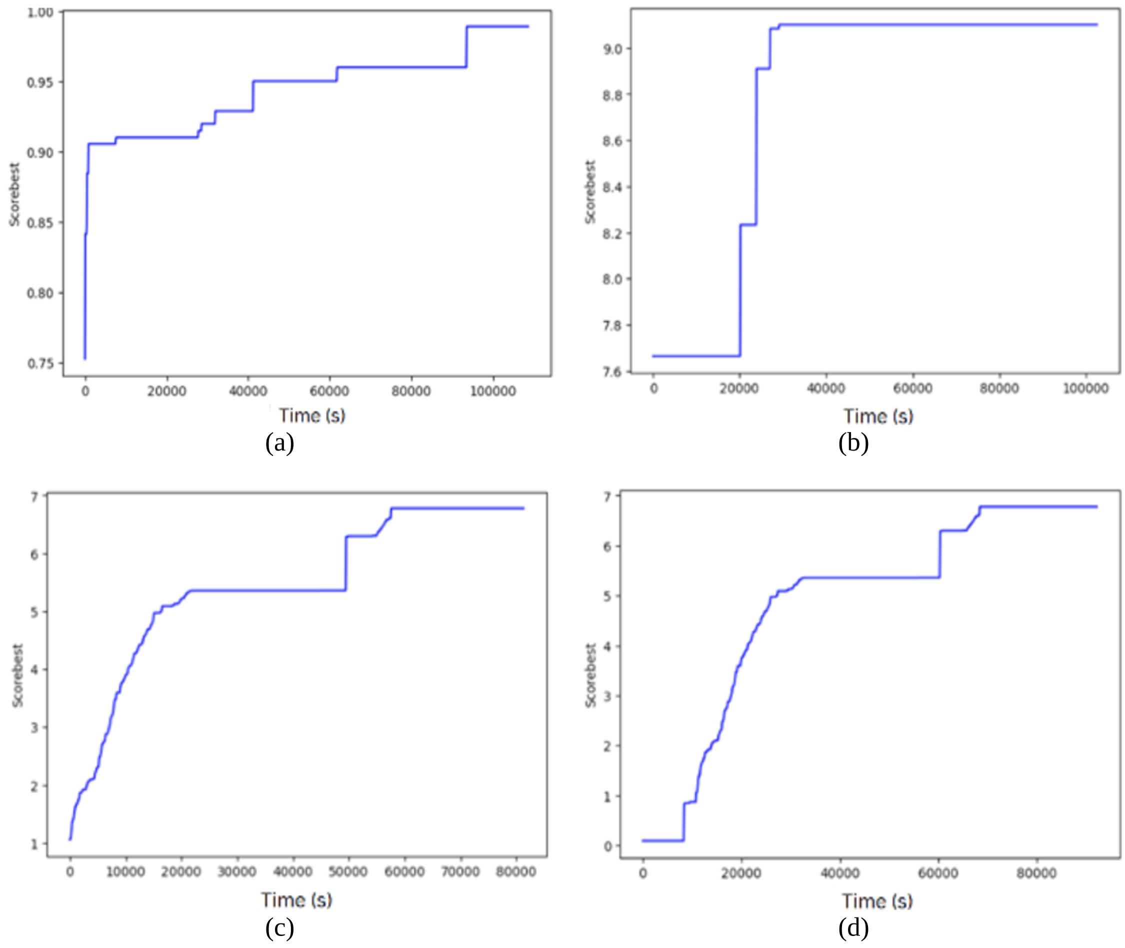

Figure 7. Convergence under different shading. (a) 0% shading, (b) 25% shading, (c) 50% shading, and (d) 75% shading

4.2.2 Tracking analysis

Tracking analysis is crucial to ensure the MPPT-AOA consistently operates close to the maximum power point. The tracking performance, as shown in Figure 8, reveals how the algorithm behaves under different shading conditions. With no shading, as shown in Figure 8(a), the MPPT-AOA maintains a stable operation near the MPP, with minimal deviations, indicating excellent tracking accuracy under optimal conditions. When shading is introduced at 25%, as shown in Figure 8(b), the system's tracking remains robust, with only slight deviations that are quickly corrected, minimizing potential power loss. However, as shading increases to 50% in Figure 8(c).

The tracking accuracy begins to suffer, with more erratic behavior due to the complex power curve. Despite these challenges, the algorithm keeps the power output within a reasonable range. In Figure 8(d), under severe shading at 75%, tracking performance declines further, with more frequent and significant deviations from the MPP. Nonetheless, the system recovers and tracks the MPP reasonably, showcasing the algorithm's resilience even under harsh conditions. This analysis suggests that while the MPPT-AOA is highly effective in maintaining optimal operation under low to moderate shading, its tracking accuracy diminishes as shading severity increases, though it performs sufficiently well.

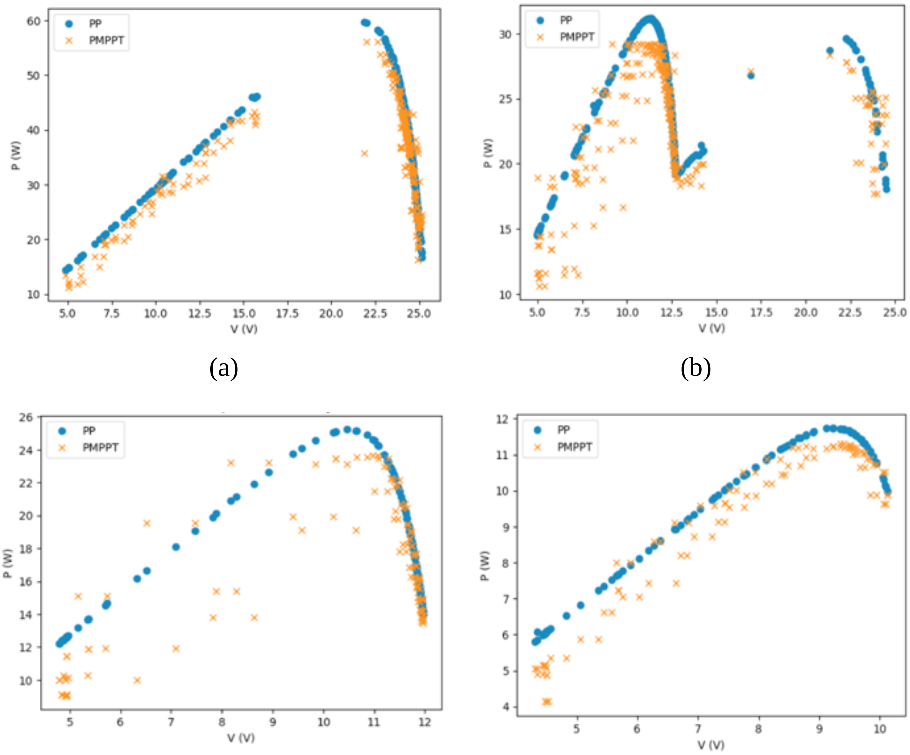

(a) (b)

(c) (d)

Figure 8. Tracking under different shading. (a) 0% shading, (b) 25% shading, (c) 50% shading, and (d) 75% shading

4.2.3. Efficiency analysis

Efficiency analysis is critical for assessing the MPPT-AOA's ability to effectively convert available solar energy into electrical power. As illustrated in Figure 9, the system's efficiency reflects its performance across varying shading conditions. It showed by Figures 9(a) to 9(d), under 0% shading, the system achieves near-optimal energy conversion with an average efficiency of 93.92%. As shading increases to 25%, there is a slight decrease in efficiency to 93.48%, which is expected as partial shading begins to impact the system's power output. At 50% shading, the efficiency drops to 92.46%, indicating the algorithm's increasing difficulty in maintaining optimal energy conversion, as shading creates more variability in the power curve. Surprisingly, even under 75% shading, the system maintains an efficiency of 92.83%, demonstrating the MPPT-AOA's effectiveness and robustness even under significant adverse conditions. The system performance also described in Table 2.

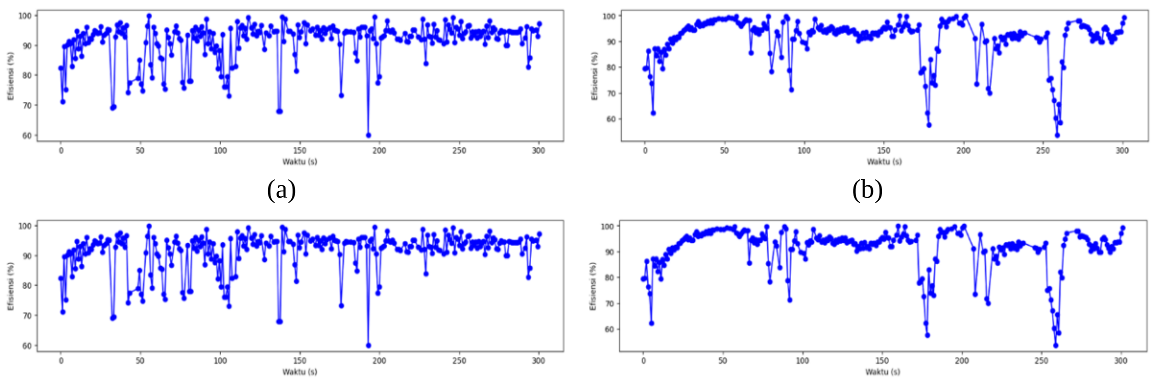

(a) (b)

(c) (d)

Figure 9. Efficiency under different shading. (a) 0% shading, (b) 25% shading, (c) 50% shading, and (d) 75% shading

Table 2. AOA-MPPT performance under different shading

Component	0% shading	25% shading	50% shading	75% shading
MPP (W)	56.03	29.21	23.67	11.30
P. Avg. (W)	34.56	23.29	16.64	9.01
Eff. Avg. (%)	93.92	93.48	92.46	92.83
Duty. Avg. (%)	18.02	37.8	38.52	39.95
MPP Obj. Val.	988535	9100575	6776146	5775146
Tracking (ms)	90.50	90.50	90.47	90.47

The consistent tracking speed across different shading levels, as indicated in Table 2, further reinforces the algorithm's reliability. The efficiency analysis shows that while the MPPT-AOA experiences minor efficiency and power output losses as shading increases, it remains a highly reliable and effective solution for maximizing energy capture in diverse environmental conditions. The system's ability to maintain high efficiency and consistent tracking performance under varying levels of shading underscores its robustness and adaptability, making it suitable for real-world applications where environmental conditions are often unpredictable.

4.3. MPPT-AOA actual condition test

This section presents the results of real-world experiments conducted to evaluate the performance of the MPPT-AOA under different environmental conditions. The study compares MPPT-AOA with the PSO algorithm and a non-MPPT system. The tests are conducted to analyze their efficiency across different daily insolation cycles and partial shading scenarios. Performance metrics such as tracking speed, power extraction efficiency, and stability are examined to assess the practical viability of MPPT-AOA.

4.3.1. Daily insolation test

The daily insolation test evaluates the performance of the MPPT-AOA, PSO, and non-MPPT systems over different daily cycles, as shown in Figure 10. The test focuses on key metrics such as maximum power (P Max), average power (P Avg), and average efficiency (Eff. Avg). Showed in Figure 10(a) to (c), the output power of the AOA-MPPT is represented by the blue lines (PMPPT), while PSO and non-MPPT systems are defined by orange lines (PPSO) and green lines (non-MPPT), respectively. In Cycle 1, the MPPT-AOA in Figure 10(a) outperforms both PSO in Figure 10(b) and non-MPPT in Figure 10(c). Achieving a maximum power of 55.31 W, compared to 53.02 W for PSO and 50.40 W for non-MPPT. The average power output for MPPT-AOA is 39.92 W, significantly higher than the 37.90 W and 36.02 W recorded by PSO and non-MPPT, respectively. The efficiency of the MPPT-AOA is also superior, with an average of 95.68%, compared to 90.12% for PSO and 85.67% for non-MPPT. This trend continues in Cycles 2 and 3, where MPPT-AOA consistently delivers higher power and efficiency, demonstrating its robustness and adaptability across different insolation conditions.

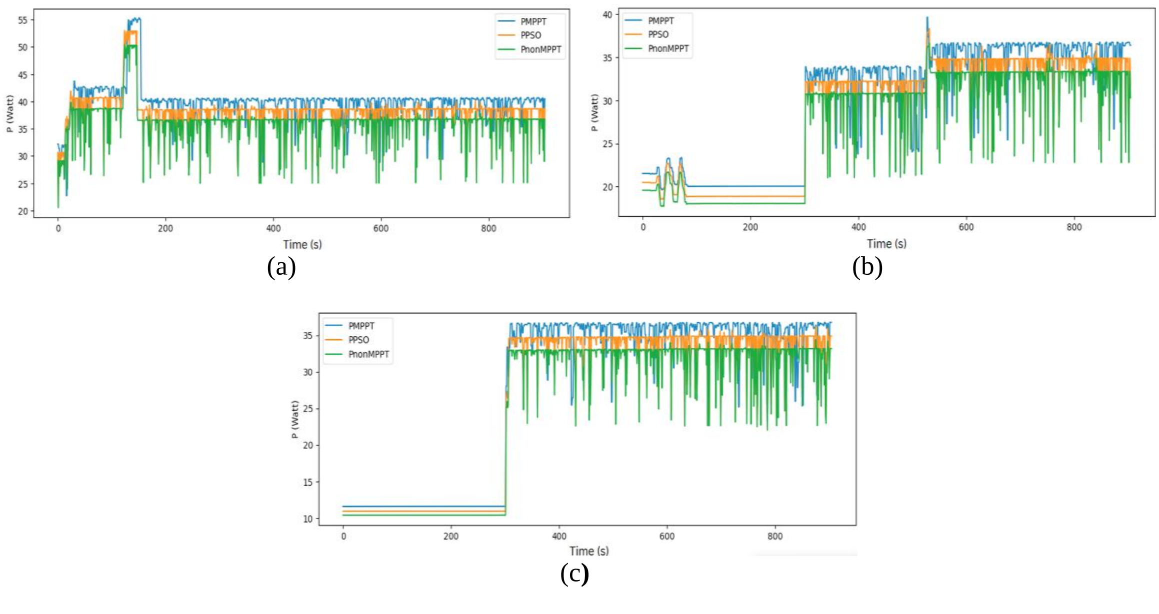

(a) (b) (c)

Figure 10. MPPT-AOA output power compared to other tested methods under different daily cycles: (a) AOA, (b) PSO, and (c) non-MPPT

The results in Table 3 further validate these observations, showing that the MPPT-AOA consistently achieves higher power and efficiency than its counterparts. In Cycle 2, the MPPT-AOA maintains a maximum power of 39.66 W and an average efficiency of 95.06%, whereas PSO and non-MPPT trail behind with lower values. Similarly, in Cycle 3, MPPT-AOA outperforms the other systems with a maximum power of 36.77 W and an efficiency of 95.62%. These findings underscore the MPPT-AOA's ability to maximize energy capture and maintain high efficiency throughout varying daily insolation cycles, making it a superior choice for real-world applications.

Table 3. AOA vs. PSO vs. Non-MPPT performance under different daily cycles

	AOA	PSO	Non-MPPT	AOA	PSO	Non-MPPT	AOA	PSO	Non-MPPT
		Cycle 1			Cycle 2			Cycle 3	
P Max. (W)	55.31	53.02	50.40	39.66	38.34	36.65	36.77	36.19	34.4
P Avg. (W)	39.92	37.90	36.02	29.62	28.29	27.04	27.27	26.06	24.76
Eff. Avg. (%)	95.68	90.12	85.67	95.06	90.11	86.14	95.62	90.12	85.64

4.3.2. Partial insolation test

The partial insolation test compares the tracking performance of MPPT-AOA, PSO, and non-MPPT systems under different shading conditions, as depicted in Figure 11. This test is crucial for understanding how well each system can adapt to partial shading, a common challenge in photovoltaic installations. Showed in Figure 11(a), the MPPT-AOA demonstrates excellent tracking accuracy under 100% irradiance, maintaining proximity to the MPP with minimal deviations. The results show that MPPT-AOA achieves an MPP of 56.03 W, with an average power output of 34.56 W and an accuracy of 93.93%. Compared, PSO and non-MPPT systems deliver lower MPPs of 52.34 W and 51.80 W, respectively, with corresponding accuracies of 87.66% and 86.75%. As shading increases to 25%, 50%, and 75%, the MPPT-AOA continues to outperform PSO and non-MPPT systems, although the gap narrows slightly. For instance, under 75% shading in Figure 11(b), the MPPT-AOA still achieves an MPP of 11.30 W, compared to 10.56 W for PSO and 10.06 W for non-MPPT. The MPPT-AOA's average power output and accuracy remain higher than those of the other systems across all shading levels. As shown in Figures 11(c) and 11(d).

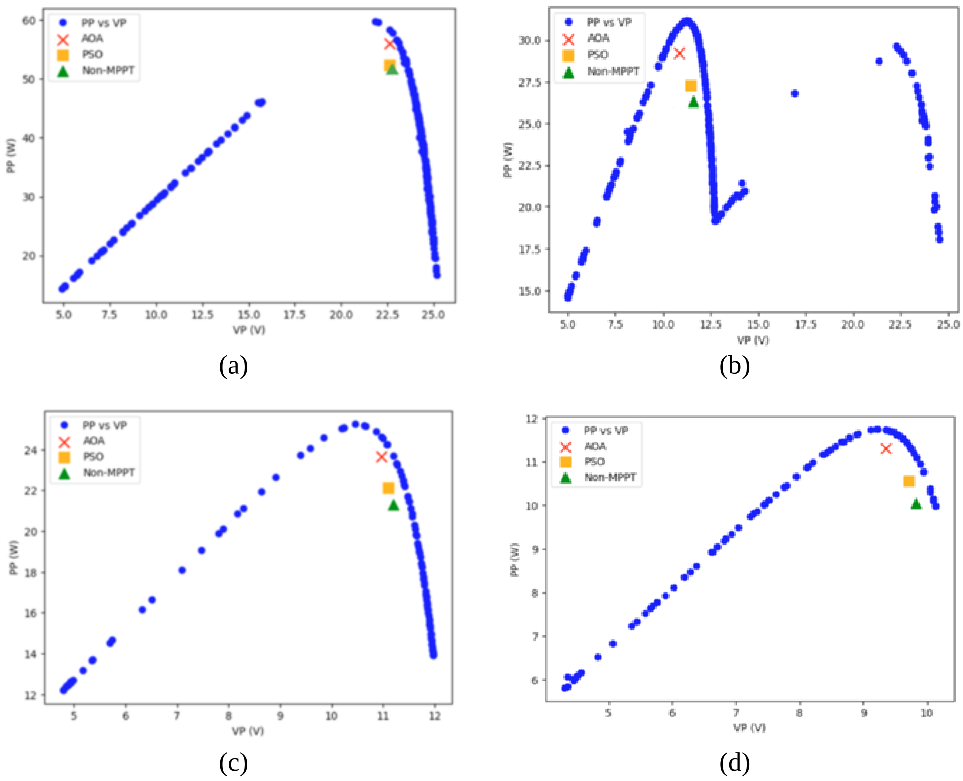

Figure 11. AOA vs. PSO vs. Non-MPPT tracking under different shading. (a) 0% shading, (b) 25% shading, (c) 50% shading, and (d) 75% shading

Table 4 provides a detailed comparison of the performance metrics under different shading conditions. The data shows that the MPPT-AOA consistently delivers higher MPP and average power, faster tracking times and greater accuracy than PSO and non-MPPT systems. In Table 4, even under the most challenging condition of 75% shading, the MPPT-AOA achieves an efficiency of 96.26%, far surpassing the efficiencies of 89.92% and 85.65% for PSO and non-MPPT, respectively. This superior performance is attributed to the adaptive nature of the AOA, which allows it to adjust to varying environmental conditions and maintain optimal performance dynamically.

Table 4. AOA vs. PSO vs. Non-MPPT performance under different shading

	MPP (W)	P. Avg (W)	Tracking (ms)	Acc. (%)
		0% shading		
AOA	56.032	34.56	90.50	93.928
PSO	52.341	32.28	100.50	87.659
NON-MPPT	51.799	32.01	-	86.751
		25% shading		
AOA	29.212	23.281	90.50	93.748
PSO	27.287	21.747	100.50	87.573
NON-MPPT	26.34	21.08	-	84.56
		50% shading		
AOA	23.76	16.64	90.53	93.742
PSO	22.11	15.54	100.53	87.568
NON-MPPT	21.31	15.15	-	84.408
		75% shading		
AOA	11.301	9.016	90.42	96.260
PSO	10.556	8.422	100.42	89.920
NON-MPPT	10.056	8.226	-	85.65

4.3.2. Comparison with existing study

The proposed AOA is evaluated against PSO, grasshopper optimization algorithm (GOA), GWO, and the Jaya algorithm to assess its performance in terms of efficiency and tracking time. Table 5 provides the results of this comparative study. The performance comparison in Table 5 reveals distinct strengths and weaknesses among the tested algorithms. The proposed AOA achieves a strong balance between high efficiency (93.1%) and fast-tracking time (0.95 seconds), making it an excellent choice for real-world photovoltaic (PV) systems requiring rapid adaptability and reliable energy extraction under partial shading conditions. While GOA (98.4%) and Jaya (98.5%) slightly outperform AOA in efficiency, their tracking times are longer (4.5 seconds for GOA and 2.4 seconds for Jaya), which could hinder responsiveness in dynamic environments. In contrast, PSO achieves moderate efficiency (87.5%) and a tracking time of 1.5 seconds, but it is outperformed by AOA in both metrics.

GWO and P&O present significant limitations. GWO, with an efficiency of 85.6% and a tracking time of 21.5 seconds, struggles to compete due to its slow response and lower energy extraction capability. Meanwhile, P&O, though the fastest algorithm (0.07 seconds), P&O has inferior efficiency (31.5%), making it unsuitable for practical applications. Based on the analysis, AOA offers the most balanced performance, excelling in efficiency and tracking speed, making it a robust and versatile solution for real-world MPPT challenges.

Table 5. Comparison of MPPT-AOA with existing study

Algorithm	Eff. (%)	Tracking (s)
AOA (Proposed)	93.1	0.95
PSO (Tested on the same hardware as AOA)	87.5	1.5
GOA [51]	98.4	4.5
GWO [51]	85.6	21.5
Jaya [52]	98.5	2.4
Marine predator algorithm (MPA) [53]	99.8	0.07
OBRL-BOA [54]	95	5.3

5. CONCLUSION

The AOA has emerged as a powerful method for achieving MPPT in PV systems, especially under challenging conditions like partial shading. Partial shading occurs when some parts of a solar panel are blocked by obstacles such as trees or buildings, leading to uneven energy production. AOA addresses this issue by efficiently finding the maximum power output point, ensuring optimal performance of the PV system. The algorithm demonstrates a remarkable efficiency rate of 93.1% and a swift tracking time of just 0.95 seconds.

Compared to other methods, such as PSO and systems without MPPT capabilities, AOA achieves significantly better results, showcasing its superior ability to adapt and perform reliably. Although algorithms like GOA and Jaya slightly surpass AOA in efficiency, AOA's faster response time makes it particularly advantageous in dynamic environments where conditions change rapidly, such as fluctuating sunlight or variable shading. Recent benchmarking studies have further compared AOA with newer methods, such as the artificial ecosystem-based optimization (AEO) and tunicate swarm algorithm (TSA), which offer high efficiency and robustness. However, AOA maintains a competitive edge due to its simplicity, lower computational requirements, and superior tracking speed, making it a practical choice for real-time applications. These findings highlight AOA as a robust, scalable, and practical solution for optimizing energy output in PV systems. Moreover, its potential extends beyond solar energy, with possibilities for broader applications in the field of renewable energy optimization, where efficiency and adaptability are crucial.

ACKNOWLEDGMENTS

The authors would like to express their sincere appreciation to the Faculty of Advanced and Multidisciplinary Technology (FTMM), Universitas Airlangga (UNAIR), and The Research Center for New and Renewable Energy Engineering, UNAIR, for their valuable facility support in conducting this research.

FUNDING INFORMATION

This research received no external funding.

AUTHOR CONTRIBUTIONS STATEMENT

This journal uses the Contributor Roles Taxonomy (CRediT) to recognize individual author contributions, reduce authorship disputes, and facilitate collaboration.

Name of Author	C	M	So	Va	Fo	I	R	D	O	E	Vi	Su	P	Fu
Sigit Dani Perkasa	✓	✓	✓			✓		✓	✓		✓			
Prisma Megantoro	✓	✓		✓			✓		✓	✓		✓		✓
Nayu Nurrohma Hidayah					✓				✓		✓		✓	
Pandi Vigneshwaran										✓		✓		

C : **C**onceptualization
M : **M**ethodology
So : **So**ftware
Va : **Va**lidation
Fo : **Fo**rmal analysis
I : **I**nvestigation
R : **R**esources
D : **D**ata Curation
O : Writing - **O**riginal Draft
E : Writing - Review & **E**diting
Vi : **Vi**sualization
Su : **Su**pervision
P : **P**roject administration
Fu : **Fu**nding acquisition

CONFLICT OF INTEREST STATEMENT

The authors declare that there is no conflict of interest regarding the publication of this manuscript.

INFORMED CONSENT

This study did not involve human participants, human data, or human tissue; therefore, informed consent was not required.

ETHICAL APPROVAL

This study did not involve human participants or animal subjects. Therefore, ethical approval was not required.

DATA AVAILABILITY

The data that support the findings of this study are available from the corresponding author, PM upon reasonable request.

REFERENCES

[1] F. Wamalwa and A. Ishimwe, "Optimal energy management in a grid-tied solar PV-battery microgrid for a public building under demand response," *Energy Reports*, vol. 12, pp. 3718–3731, 2024, doi: 10.1016/j.egyr.2024.09.054.

[2] P. Megantoro, I. E. Prabowo, and M. A. Shomad, "Development of maximum power point tracking solar charge controller for 120-volt battery system at pandansimo hybrid power plant," *Journal of Physics: Conference Series*, vol. 1471, no. 1, Feb. 2020, doi: 10.1088/1742-6596/1471/1/012047.

[3] S. Sarkar, K. Uma Rao, V. Prema, M. S. Bhaskar, S. Padmanaban, and J. Bhargav, "A model for effect of partial shading on PV panels with experimental validation," *Energy Reports*, vol. 12, pp. 3460–3469, 2024, doi: 10.1016/j.egyr.2024.09.015.

[4] P. Ramesh, R. K. Pongiannan, L. Demel, R. Hrbac, and N. R, "Maximum efficiency and power point tracking system for hybrid compensated wireless charging of electric vehicle," *Results in Engineering*, vol. 25, p. 104100, Mar. 2025, doi: 10.1016/j.rineng.2025.104100.

[5] A. Z. Arsad, A. W. M. Zuhdi, A. D. Azhar, C. F. Chau, and A. Ghazali, "Advancements in maximum power point tracking for solar charge controllers," *Renewable and Sustainable Energy Reviews*, vol. 210, 2025, doi: 10.1016/j.rser.2024.115208.

[6] P. Megantoro, F. Danang Wijaya, and E. Firmansyah, "Analyze and optimization of genetic algorithm implemented on maximum power point tracking technique for PV system," in *2017 International Seminar on Application for Technology of Information and Communication (iSemantic)*, Oct. 2017, pp. 79–84. doi: 10.1109/ISEMANTIC.2017.8251847.

[7] P. Megantoro, Y. D. Nugroho, F. Anggara, Suhono, and E. Y. Rusadi, "Simulation and characterization of genetic algorithm implemented on MPPT for PV system under partial shading condition," in *2018 3rd International Conference on Information Technology, Information System and Electrical Engineering (ICITISEE)*, Nov. 2018, pp. 74–78. doi: 10.1109/ICITISEE.2018.8721031.

[8] M. A. Zeddini, S. Krim, and M. F. Mimouni, "Experimental validation of an advanced metaheuristic algorithm for maximum power point tracking of a shaded photovoltaic system: A comparative study between three approaches," *Energy Reports*, vol. 10, pp. 161–185, Nov. 2023, doi: 10.1016/j.egyr.2023.06.019.

[9] N. Mallick, C. K. Shiva, and V. Mukherjee, "Novel optimized closed-loop fuzzy control for maximum power tracking of proton exchange membrane fuel cell," *Results in Engineering*, vol. 25, p. 104303, Mar. 2025, doi: 10.1016/j.rineng.2025.104303.

[10] U. Yilmaz, A. Kircay, and S. Borekci, "PV system fuzzy logic MPPT method and PI control as a charge controller," *Renewable and Sustainable Energy Reviews*, vol. 81, pp. 994–1001, Jan. 2018, doi: 10.1016/j.rser.2017.08.048.

[11] Q. Zhou, J. Jin, and R. Yang, "Static state power smoothing and transient power quality enhancement of a DC microgrid based on multi-function SMES/battery distributed hybrid energy storage system," *Energy Reports*, vol. 8, pp. 44–51, Nov. 2022, doi: 10.1016/j.egyr.2022.08.051.

[12] M. Naiem-Ur-Rahman *et al.*, "An asymmetric fuzzy-based self-tuned PSO-Optimized MPPT controller for grid-connected solar photovoltaic system," *Energy Conversion and Management: X*, vol. 26, p. 100902, Apr. 2025, doi: 10.1016/j.ecmx.2025.100902.

[13] R. Chaibi, R. EL Bachtiri, K. El Hammoumi, and M. Yagoubi, "Observer-based fuzzy T–S control with an estimation error guarantee for MPPT of a photovoltaic battery charger in partial shade conditions," *Results in Control and Optimization*, vol. 17, p. 100488, Dec. 2024, doi: 10.1016/j.rico.2024.100488.

[14] M. Mohammadinodoushan, R. Abbassi, H. Jerbi, F. Waly Ahmed, H. kh ahmed, and A. Rezvani, "A new MPPT design using variable step size perturb and observe method for PV system under partially shaded conditions by modified shuffled frog leaping algorithm- SMC controller," *Sustainable Energy Technologies and Assessments*, vol. 45, Jun. 2021, doi: 10.1016/j.seta.2021.101056.

[15] L. G. K. Chai, L. Gopal, F. H. Juwono, C. W. R. Chiong, H.-C. Ling, and T. A. Basuki, "A novel global MPPT technique using improved PS-FW algorithm for PV system under partial shading conditions," *Energy Conversion and Management*, vol. 246, Oct. 2021, doi: 10.1016/j.enconman.2021.114639.

[16] M. E. Girgis and N. A. Elkhateeb, "Enhancing photovoltaic MPPT with P& O algorithm performance based on adaptive PID control using exponential forgetting recursive least squares method," *Renewable Energy*, vol. 237, p. 121801, Dec. 2024, doi: 10.1016/j.renene.2024.121801.

[17] H. Chaieb and A. Sakly, "A novel MPPT method for photovoltaic application under partial shaded conditions," *Solar Energy*, vol. 159, pp. 291–299, Jan. 2018, doi: 10.1016/j.solener.2017.11.001.

[18] A.-M. Badea, D. Manaila-Maximean, L. Fara, and D. Craciunescu, "Maximizing solar photovoltaic energy efficiency: MPPT techniques investigation based on shading effects," *Solar Energy*, vol. 285, p. 113082, Jan. 2025, doi: 10.1016/j.solener.2024.113082.

[19] J. G. Njiri, Y. Liu, and D. Söffker, "Multivariable control of large variable-speed wind turbines for generator power regulation and load reduction," *IFAC-PapersOnLine*, vol. 48, no. 1, pp. 544–549, 2015, doi: 10.1016/j.ifacol.2015.05.035.

[20] R. K. Jain, H. K. V. Gadiraju, V. R. Barry, and S. R. Parne, "High performance MPPT controller based on adaptive sliding mode control," in *2020 21st National Power Systems Conference (NPSC)*, Dec. 2020, pp. 1–6. doi: 10.1109/npsc49263.2020.9331826.

[21] M. I. Mosaad, M. O. Abed el-Raouf, M. A. Al-Ahmar, and F. A. Banakher, "Maximum power point tracking of PV system based cuckoo search algorithm; review and comparison," *Energy Procedia*, vol. 162, pp. 117–126, Apr. 2019, doi: 10.1016/j.egypro.2019.04.013.

[22] H. Belmadani *et al.*, "Guided seagull optimization for improved PV MPPT in partial shading," in *2023 IEEE 3rd International Conference on Applied Electromagnetics, Signal Processing, & Communication (AESPC)*, Nov. 2023, pp. 1–5. doi: 10.1109/aespc59761.2023.10390053.

[23] K. T. Swetha, V. R. Barry, A. Robinson, and R. K. Jain, "A Novel Spotted Hyena Optimization algorithm for MPPT under Partial Shading Conditions," in *IECON 2021 – 47th Annual Conference of the IEEE Industrial Electronics Society*, Oct. 2021, pp. 1–6. doi: 10.1109/iecon48115.2021.9589790.

[24] D. Fares, M. Fathi, I. Shams, and S. Mekhilef, "A novel global MPPT technique based on squirrel search algorithm for PV module under partial shading conditions," *Energy Conversion and Management*, vol. 230, Feb. 2021, doi: 10.1016/j.enconman.2020.113773.

[25] T. Thi Hoang and T. Huong Le, "Application of mutant particle swarm optimization for MPPT in photovoltaic system," *Indonesian Journal of Electrical Engineering and Computer Science*, vol. 19, no. 2, pp. 600–607, Aug. 2020, doi: 10.11591/ijeecs.v19.i2.pp600-607.

[26] X. Li, Z. Youzhuo, H. Wei, Z. Shuyi, Z. Wenqiang, and C. Haobin, "Control strategy for photovoltaic array MPPT based on an improved particle swarm optimization algorithm," in *2024 9th Asia Conference on Power and Electrical Engineering (ACPEE)*, Apr. 2024. doi: 10.1109/acpee60788.2024.10532728.

[27] Y.-P. Huang, M.-Y. Huang, and C.-E. Ye, "A fusion firefly algorithm with simplified propagation for Photovoltaic MPPT under partial shading conditions," *IEEE Transactions on Sustainable Energy*, vol. 11, no. 4, pp. 2641–2652, Oct. 2020, doi: 10.1109/TSTE.2020.2968752.

[28] M. Zhang, Z. Chen, and L. Wei, “An immune firefly algorithm for tracking the maximum power point of PV array under partial shading conditions,” *Energies*, vol. 12, no. 16, Aug. 2019, doi: 10.3390/en12163083.

[29] S. Mohanty, B. Subudhi, and P. K. Ray, “A new MPPT design using grey wolf optimization technique for photovoltaic system under partial shading conditions,” *IEEE Transactions on Sustainable Energy*, vol. 7, no. 1, pp. 181–188, Jan. 2016, doi: 10.1109/TSTE.2015.2482120.

[30] M. Mansoor, A. F. Mirza, and Q. Ling, “Harris hawk optimization-based MPPT control for PV systems under partial shading conditions,” *Journal of Cleaner Production*, vol. 274, Nov. 2020, doi: 10.1016/j.jclepro.2020.122857.

[31] M. S. Bouakkaz *et al.*, “Dynamic performance evaluation and improvement of PV energy generation systems using moth flame optimization with combined fractional order PID and sliding mode controller,” *Solar Energy*, vol. 199, pp. 411–424, Mar. 2020, doi: 10.1016/j.solener.2020.02.055.

[32] M. Mansoor, A. F. Mirza, Q. Ling, and M. Y. Javed, “Novel grass hopper optimization based MPPT of PV systems for complex partial shading conditions,” *Solar Energy*, vol. 198, pp. 499–518, Mar. 2020, doi: 10.1016/j.solener.2020.01.070.

[33] S. Titri, C. Larbes, K. Y. Toumi, and K. Benatchba, “A new MPPT controller based on the Ant colony optimization algorithm for Photovoltaic systems under partial shading conditions,” *Applied Soft Computing*, vol. 58, pp. 465–479, Sep. 2017, doi: 10.1016/j.asoc.2017.05.017.

[34] M. Hamza Zafar *et al.*, “A novel meta-heuristic optimization algorithm based MPPT control technique for PV systems under complex partial shading condition,” *Sustainable Energy Technologies and Assessments*, vol. 47, Oct. 2021, doi: 10.1016/j.seta.2021.101367.

[35] P. Megantoro, H. F. Aldi Kusuma, L. J. Awalin, Y. Afif, D. F. Priambodo, and P. Vigneshwaran, “Comparative analysis of evolutionary-based maximum power point tracking for partial shaded photovoltaic,” *International Journal of Electrical and Computer Engineering (IJECE)*, vol. 12, no. 6, pp. 5717–5729, Dec. 2022, doi: 10.11591/ijece.v12i6.pp5717-5729.

[36] L. Fan, Q. Chen, and Z. Guo, “An Fuzzy improved perturb and observe (P&O) maximum power point tracking (MPPT) algorithm for microbial fuel cells,” *International Journal of Electrochemical Science*, vol. 17, no. 11, p. 221157, Nov. 2022, doi: 10.20964/2022.11.49.

[37] H. Krishnan, M. S. Islam, M. A. Ahmad, and M. I. M. Rashid, “Parameter identification of solar cells using improved Archimedes optimization algorithm,” *Optik*, vol. 295, Dec. 2023, doi: 10.1016/j.ijleo.2023.171465.

[38] S.-J. Jiang, S.-C. Chu, F.-M. Zou, J. Shan, S.-G. Zheng, and J.-S. Pan, “A parallel Archimedes optimization algorithm based on Taguchi method for application in the control of variable pitch wind turbine,” *Mathematics and Computers in Simulation*, vol. 203, pp. 306–327, Jan. 2023, doi: 10.1016/j.matcom.2022.06.027.

[39] I. Sajid, A. Sarwar, M. Tariq, F. I. Bakhsh, S. Ahmad, and A. Shah Noor Mohamed, “Archimedes optimization algorithm (AOA)-based global maximum power point tracking for a photovoltaic system under partial and complex shading conditions,” *Energy*, vol. 283, Nov. 2023, doi: 10.1016/j.energy.2023.129169.

[40] L. K. Fong, M. S. Islam, and M. A. Ahmad, “Optimized PID controller of DC-DC buck converter based on Archimedes optimization algorithm,” *International Journal of Robotics and Control Systems*, vol. 3, no. 4, pp. 658–672, Sep. 2023, doi: 10.31763/ijrcs.v3i4.1113.

[41] M. Nurmuhammed, O. Akdağ, and T. Karadağ, “A novel modified Archimedes optimization algorithm for optimal placement of electric vehicle charging stations in distribution networks,” *Alexandria Engineering Journal*, vol. 84, pp. 81–92, Dec. 2023, doi: 10.1016/j.aej.2023.10.055.

[42] I. M. Mehedi *et al.*, “Critical evaluation and review of partial shading mitigation methods for grid-connected PV system using hardware solutions: The module-level and array-level approaches,” *Renewable and Sustainable Energy Reviews*, vol. 146, Aug. 2021, doi: 10.1016/j.rser.2021.111138.

[43] M. N. R. Nazeri, M. F. N. Tajuddin, T. S. Babu, A. Azmi, M. Malvoni, and N. M. Kumar, “Firefly algorithm-based photovoltaic array reconfiguration for maximum power extraction during mismatch conditions,” *Sustainability*, vol. 13, no. 6, Mar. 2021, doi: 10.3390/su13063206.

[44] S. Sugumar, D. Prince Winston, and M. Pravin, “A novel on-time partial shading detection technique for electrical reconfiguration in solar PV system,” *Solar Energy*, vol. 225, pp. 1009–1025, Sep. 2021, doi: 10.1016/j.solener.2021.07.069.

[45] T.-T. Nguyen, T.-K. Dao, T.-T.-T. Nguyen, and T.-D. Nguyen, “An optimal microgrid operations planning using improved Archimedes optimization algorithm,” *IEEE Access*, vol. 10, pp. 67940–67957, 2022, doi: 10.1109/ACCESS.2022.3185737.

[46] F. A. Hashim, K. Hussain, E. H. Houssein, M. S. Mabrouk, and W. Al-Atabany, “Archimedes optimization algorithm: a new metaheuristic algorithm for solving optimization problems,” *Applied Intelligence*, vol. 51, no. 3, pp. 1531–1551, Mar. 2021, doi: 10.1007/s10489-020-01893-z.

[47] M. Nurmuhammed, O. Akdağ, and T. Karadağ, “Modified archimedes optimization algorithm for global optimization problems: a comparative study,” *Neural Computing and Applications*, vol. 36, no. 14, pp. 8007–8038, May 2024, doi: 10.1007/s00521-024-09497-1.

[48] A. Fathy, A. G. Alharbi, S. Alshammari, and H. M. Hasanien, “Archimedes optimization algorithm based maximum power point tracker for wind energy generation system,” *Ain Shams Engineering Journal*, vol. 13, no. 2, Mar. 2022, doi: 10.1016/j.asej.2021.06.032.

[49] H. A. A. Hannon, A. T. Abdulsadda, and H. K. Latif, “Archimedes optimization algorithm based extremum seeking control maximum power point tracking for enhancing performance and efficiency of photovoltaic systems,” in *AIP Conference Proceedings*, 2023. doi: 10.1063/5.0137307.

[50] J. Liu, M. Yang, and W. Tao, “Impedance-Based Stability Analysis of Grid-Tied Photovoltaic System With Superconducting Magnetic Energy Storage System,” *IEEE Transactions on Applied Superconductivity*, vol. 31, no. 8, pp. 1–4, Nov. 2021, doi: 10.1109/tasc.2021.3101778.

[51] R. Sridhar, S. Jeevananthan, S. S. Dash, and P. Vishnuram, “A new maximum power tracking in PV system during partially shaded conditions based on shuffled frog leap algorithm,” *Journal of Experimental & Theoretical Artificial Intelligence*, vol. 29, no. 3, pp. 481–493, May 2017, doi: 10.1080/0952813X.2016.1186750.

[52] K. T. Swetha and V. R. Barry, “Modified jaya algorithm for photovoltaic power tracking under partial shading conditions,” in *2021 National Power Electronics Conference (NPEC)*, Dec. 2021, pp. 1–5. doi: 10.1109/npec52100.2021.9672524.

[53] S. K. Vankadara, S. Chatterjee, P. K. Balachandran, and L. Mihet-Popa, “Marine predator algorithm (MPA)-based MPPT technique for solar PV systems under partial shading conditions,” *Energies*, vol. 15, no. 17, Aug. 2022, doi: 10.3390/en15176172.

[54] B. Aljafari, P. K. Balachandran, D. Samithas, and S. B. Thanikanti, “Solar photovoltaic converter controller using opposition-based reinforcement learning with butterfly optimization algorithm under partial shading conditions,” *Environmental Science and Pollution Research*, vol. 30, no. 28, pp. 72617–72640, May 2023, doi: 10.1007/s11356-023-27261-1.

BIOGRAPHIES OF AUTHORS

Sigit Dani Perkasa is graduated from electrical engineering at Universitas Airlangga in 2024. He actively researches renewable energy, control systems, optimization systems, instrumentation, and microcontroller systems as a part of Universitas Airlangga's Research Centre for New and Renewable Energy Engineering (RCNREE). He can be contacted at the following email: sigit.dani.perkasa-2020@ftmm.unair.ac.id.

Prisma Megantoro has been an electrical engineering lecturer at the Faculty of Advanced Technology and Multidiscipline, Universitas Airlangga (UNAIR), Surabaya, Indonesia, since 2020. He founded the research center for new and renewable energy engineering (RCeNREE) UNAIR. He received his bachelor's and master's degrees from Universitas Gadjah Mada, Yogyakarta, Indonesia, in 2014 and 2018. His current research is focused on renewable energy systems, solar photovoltaic engineering, embedded systems, and the internet of things. He can be contacted at the following email: prisma.megantoro@ftmm.unair.ac.id.

Nayu Nurrohma Hidayah is a seventh-semester undergraduate student majoring in electrical engineering at Universitas Airlangga. She actively researches renewable energy, instrumentation, and power systems as a part of Universitas Airlangga's research center for new and renewable energy engineering (RCNREE). She can be contacted at email: nayu.nurrohma.hidayah-2021@ftmm.unair.ac.id.

Pandi Vigneshwaran obtained his doctoral degree from Anna University Chennai in 2016 and his Master of Engineering from Anna University Chennai in June 2005. He has more than 20 years of experience and specialization in Cybersecurity. Presently, He is working as a Professor in the Department of Computer Science and Engineering at Acharya University, Karakul, Uzbekistan. His area of interest includes security, routing, and intelligent data analysis. He can be contacted at email: vigneshwaran05@gmail.com.